RAA 2016 Vol. **16** No. **2**, 32 (8pp) doi: 10.1088/1674–4527/16/2/032
http://www.raa-journal.org *http://iopscience.iop.org/raa*

***R**esearch in*
***A**stronomy and*
***A**strophysics*

Energy spectral property in an isolated CME-driven shock

Xin Wang[1,2,3,4], Yi-Hua Yan[2], Ming-De Ding[3], Na Wang[1,4] and Hao Shan[1,4]

[1] Xinjiang Astronomical Observatory, Chinese Academy of Sciences, Urumqi 830011, China; *wangxin@xao.ac.cn*

[2] Key Laboratory of Solar Activity, National Astronomical Observatories, Chinese Academy of Sciences, Beijing 100012, China

[3] Key Laboratory of Modern Astronomy and Astrophysics (Nanjing University), Ministry of Education, Nanjing 210093, China

[4] Key Laboratory of Radio Astronomy, Chinese Academy of Sciences, Nanjing 210008, China

Received 2015 July 8; accepted 2015 September 10

Abstract Observations from multiple spacecraft show that there are energy spectral "breaks" at 1–10 MeV in some large CME-driven shocks. However, numerical models can hardly simulate this property due to high computational expense. The present paper focuses on analyzing these energy spectral "breaks" by Monte Carlo particle simulations of an isolated CME-driven shock. Taking the 2006 Dec 14 CME-driven shock as an example, we investigate the formation of this energy spectral property. For this purpose, we apply different values for the scattering time in our isolated shock model to obtain the highest energy "tails," which can potentially exceed the "break" energy range. However, we have not found the highest energy "tails" beyond the "break" energy range, but instead find that the highest energy "tails" reach saturation near the range of energy at 5 MeV. So, we believe that there exists an energy spectral "cut off" in an isolated shock. If there is no interaction with another shock, there would not be formation of the energy spectral "break" property.

Key words: acceleration of particles — shock waves — Sun: coronal mass ejections (CMEs) — solar wind — methods: numerical

1 INTRODUCTION

Strong astrophysical shocks are often associated with superthermal particle emission and with magnetic field amplification (Bykov et al. 2013; Vladimirov et al. 2006). This phenomenon suggests that shocks are regions where particles are efficiently accelerated, and this large group of energetic particles is responsible for the excitation of magnetic turbulence via plasma instabilities (Bell 1978; Bell et al. 2013; Jokipii 2013). These magnetic fields which diffuse cosmic rays in the vicinity of the shock are required to be much higher than the averaged magnetic field in the interstellar medium.

The theoretical model includes the determination of the particle injection energy from the thermal particle distribution into the non-thermal particle distribution, the maximum energy of particles accelerated at the shock, energetic particle spectra at all spatial and temporal locations, and the dynamical distribution of particles that escape upstream and downstream from the evolving shock complex (Zank et al. 2000). Monte Carlo simulation results indicate that solar ejecta transfers energy into the non-thermal particles in an interplanetary shock with an efficiency of $\sim$ 10% (Wang et al. 2013). Studies of the dependence of this efficiency on the angle between shock normal and the magnetic field direction (θ_{BN}) can have implications for ground-level enhancement events (Li et al. 2010; Snodin et al. 2013). Estimation of the maximum particle energy by coronal mass ejection (CME)-driven shocks is becoming more and more vital for forecasting space weather. Since particles accelerated at the shock escape rather easily from the acceleration site, they can be detected well before the arrival of the shock. This, of course, has immediate and interesting implications for space weather monitoring and prediction systems, but it also implies that the study of the ion acceleration mechanism is complicated by the subsequent interplanetary propagation of the energetic particles.

For the past several decades, there has been much literature focusing on all aspects of the diffusive shock acceleration (DSA). In the past, cosmic ray (CR) spectra, acceleration efficiency, and amplification of the magnetic field have been calculated regularly via a two-fluid approach (Drury 1983). More recently, those have been simulated via a particle Monte Carlo method (Vladimirov et al. 2006; Wang & Yan 2011; Ellison & Double 2004; Ellison et al. 1990; Niemiec & Ostrowski 2004), via a hybrid method (Caprioli & Spitkovsky 2014; Gargaté & Spitkovsky 2012; Giacalone et al. 1993; Guo & Giacalone 2013; Winske 1985), or via a full particle-in-cell (PIC) method (Amano & Hoshino 2007; Riquelme & Spitkovsky 2011). In addi-

tion, the CR's transport equations have also been solved by a numerical method (Kang et al. 2002; Zirakashvili & Aharonian 2010) and an analytical method (Liu et al. 2004; Caprioli et al. 2010; Malkov & Voelk 1996). These methods are all able to provide consistent results for the dynamics of the shock including the CR's back-reaction. However, unlike the analytical method, the particle method and the numerical MHD method have not yet been able to simulate the energy spectral "break" property (Malkov et al. 2013). Since the "break" of the energy spectrum would be associated with the particle leakage mechanism, Malkov has presented a new combined diffusion coefficient to describe particle acceleration and escape in different regions. It accounts for a highly turbulent magnetic field in the vicinity of the shock site (particle acceleration) and for faded turbulence of the magnetic field far from the shock front (particle escape).

Although it is widely accepted that the most efficient acceleration of solar energetic particles (SEPs) would happen in CME-driven shocks, the underlying acceleration mechanism in the shock environment still remains uncertain. In particular, it is not clear how the extensive maximum particle energy can be produced or why the energy spectral shape can be broken (i.e., why an abrupt change in the slope of the energy spectrum can occur) in some large CME-driven shocks (Mewaldt et al. 2008). In the past solar cycle 23, there were several observed events exhibiting proton energy spectral "breaks." These events occurred on 1997 Nov 6, 2001 Apr 15, 2005 Jan 20, 2005 Sep 7, 2006 Dec 05, and 2006 Dec14. In addition, there are hard X-ray and γ-ray energy spectra from the Reuven Ramaty High Energy Solar Spectroscopic Imager (RHESSI) that were recorded on 2002 July 23. This event shows a double-power-law spectrum with a "break" at ~ 30 keV in X-ray and a high energy "cut-off" tail at $\sim$5 MeV in γ-ray. The X-ray spectrum indicates that substantial electron acceleration reached tens of keV. The γ-ray line showed that ions were accelerated to tens of MeV (Lin et al. 2003). There were also some debates about a broken lower energy spectrum in X-ray, which is far different from an ad hoc assumption of hot thermal plasma displaying the highest low-energy cutoff ($\sim$20 keV). Actually, there are a lot of analyses of the hardening spectra in the energy range varying from 20 keV to a few MeV (Gan et al. 2001; Kong et al. 2013; Huang 2009). In more recent years, an extensive SEP event was detected by STEREO A on 2012 July 23 near 1 AU. Liu et al. (2014) suggest that the in-transit interaction between two closely launched CMEs resulted in the extreme enhancement of the SEP event. These results provide a new view crucial to space weather and solar physics as to how an extreme space weather event can be produced from an interaction between solar energetic ejecta (Gopalswamy et al. 2005; Cheng et al. 2013; Wang & Ji 2013; Su et al. 2013; Schneider 1993).

The parallel shocks show an effective amplification of the initial magnetic field due to the current of energetic ions that propagate anisotropically into the upstream flow. Caprioli & Spitkovsky (2013, 2014) have used 2D and 3D hybrid simulations with large computational boxes to reveal the formation of upstream filaments and cavities, which eventually trigger the Richtmeyer–Meshkov instability at the shock, and lead to further turbulent amplification of magnetic fields in the downstream region. The typical acceleration time, up to energy E in a shock with velocity $v_{\rm sh}$, is of order $T_{\rm acc} \approx D(E)/v_{\rm sh}^2$ (Drury 1983), where $D(E)$ is the diffusion coefficient. The acceleration characteristic timescale would be roughly equivalent to the timescale of the ejecta-dominated stage: when the shock is formed, the shock velocity drops quite rapidly, and so does amplification of the magnetic field (Guo & Giacalone 2012). In a certain acceleration timescale of the shock system, the maximum particle energy is decided. However, in the particle simulation system, the particle's free escape boundary (FEB) size should be considered, which means the highest energy particle would escape from the FEB. If the present simulation focuses on production of the maximum particle energy, the highest energy spectral "tail" should be preserved. To obtain the maximum particle energy, we can either add the FEB size or decrease the value for the scattering time. Due to the expansion of the FEB size, the shock system will cause an extra computational burden, so we can change the value for the scattering time. In the amplified magnetic field with an order of magnitude $\delta B/B_0 \sim 1$, the scattering time is an important factor to determine the acceleration efficiency in the resonant diffusion condition, and thereby determine if the maximum particle energy can be achieved. In this isolated shock model, we can investigate the maximum particle energy by changing the value for the scattering time.

Because we are not sure if an isolated CME-driven shock can accelerate energetic particles beyond $E_{\rm break}$ and even up to GeV, we take an isolated shock as an example to investigate the maximum particle energy and energy spectral "break" by using different values for the scattering time within resonant diffusive scenarios. According to DSA theory, acceleration efficiency is significantly enhanced once the mean free path for pitch-angle scattering is approximately equal to the particle's gyroradius (i.e. $\lambda \approx r_L(E) \propto E/B$), and the diffusion coefficient reads $D_B(E) \approx v r_L(E)$ (Lagage & Cesarsky 1983). If the Bohm diffusion condition is satisfied in the shock system and there is a typical interplanetary magnetic field with an order of a few mG, one can estimate that the maximum particle energy would be $E_{\rm max} \approx 1$ MeV, which is not enough to explain the energy spectral "break" at 1–10 MeV in observations (Ellison et al. 1990). Therefore, we hope to extensively calculate the maximum particle energy $E_{\rm max}$ using different values for the scattering time within an isolated shock model. If we can obtain $E_{\rm max} > E_{\rm break}$, this would imply that it is unnecessary to use a multiple shock model to explain the energy spectral "break" property. If we obtain $E_{\rm max} < E_{\rm break}$, then we should examine whether there is an energy spectral "break" at $E_{\rm break}$ and whether we should apply a multiple shock model.

In the present paper, we do simulations to further investigate the maximum particle energy in an isolated CME shock by using different values for the scattering time. In Section 2, we briefly introduce the dynamical Monte Carlo simulation method. In Section 3, the simulated results and analysis are presented. In the end, Section 4, we give a summary and some conclusions.

2 METHOD

Many deviations of DSA arise from the nonlinear effects of the shock, such as modification of the shock structure, magnetic field obliquity, time-dependence, magnetic field amplification, etc. Those have been calculated by a two-fluid model (Drury & Voelk 1981), an analytical model (Caprioli et al. 2010; Malkov & Voelk 1996; Amato & Blasi 2006) and particle models including hybrid, PIC and the Monte Carlo method (Gargaté & Spitkovsky 2012; Giacalone 2004; Amano & Hoshino 2007; Riquelme & Spitkovsky 2011; Vladimirov et al. 2006; Ellison & Double 2004; Wang & Yan 2011). These models return consistent results and can also provide results on the dynamics of the shock including the CR's back-reactions. In general, there are two aspects in the deviation of DSA: one aspect is about the issue of transfer depending on the macro factors of the shock including Mach number, magnetic field obliquity, time dependence, etc; another aspect is about the issue of how acceleration depends on micro factors of the shock including diffusive coefficient, injection rate, scattering time, etc.

Here, we use a dynamical Monte Carlo method to study how acceleration depends on the factor of scattering time. In this isolated shock model, the maximum particle energy $E_{\max}$ will be calculated in different cases by applying different values for the constant of the scattering time. Since the FEB measures the size of the faded turbulent magnetic field in the shock precursor region, if the FEB size is larger, then $E_{\max}$ is higher. Unfortunately, if the size of the FEB is larger, then the computational expense is higher. Instead, we can change the scattering time to achieve a higher $E_{\max}$ in the shock. Assuming a particle can obtain the same additional energy gain from each cycle in a period of the scattering time, it is probable that higher scattering probabilities will obtain more energy gains. If we take a smaller value for the constant of the scattering time in one simulation case, we can obtain a higher value of $E_{\max}$ by increasing the scattering probabilities during the simulation.

Although there is still the impact from the diffusive coefficient in different shock regions, it can be neglected in this isolated shock model. Since the ejecta moves with a large speed and the majority of accelerated particles are located in the turbulent magnetic field in the vicinity of ejecta, the diffusive processes can always be described by the Bohm condition and the difference in its coefficient in this limited precursor region would be slight.

The Monte Carlo approach regards the fluid as being composed of particles and focuses on the scattering micro processes between the particles and turbulent magnetic field in the diffusion processes. This technique is based on computational grids, where a large number of particles are distributed. A particle's mean free path is proportional to its local velocity in its local frame as follows.

$$\lambda = \upsilon_L \cdot \tau \,, \tag{1}$$

where υ_L is the local velocity of particles and τ is the scattering time. In Earth's bow shock model, the scattering time τ is taken as a constant (Knerr et al. 1996). For comparing values of maximum particle energy $E_{\max}$, we apply different values for the constant of the scattering time to perform these corresponding cases as in Table 1. To simulate the scattering processes accurately, the scattering time τ should be chosen to be far more than time step dt as follows.

$$\tau \gg dt \,. \tag{2}$$

To simulate the shock's formation and evolution, we set the standard scattering time τ_0 as a constant for all particles in Case A. Other constants of the scattering time and corresponding cases can be seen in Table 1. Those related simulation parameters can be referenced in previous work (Wang & Yan 2012). Here, we just list the scattering times in different cases. All of the scattering times are chosen to be more than time step dt ($dt = \tau_0/25$) in the corresponding cases.

Table 1 Six Cases with Corresponding Constants of the Scattering Time

Simulation cases	A	B	C	D	E	F
The scattering time	τ_0	$\tau_0/2$	$\tau_0/3$	$\tau_0/4$	$\tau_0/5$	$\tau_0/12.5$

3 RESULTS

3.1 Acceleration of Particles

To inspect the acceleration processes of particles in the shock, we extract a number of representative particles from the simulated box in each case. Six plots in Figure 1 are taken from six simulated cases labeled Cases A, B, C, D, E and F, respectively. Each curve in each plot represents one particle's evolution of velocity and energy with time. Every plot has a few peak velocities in some accelerated particles, and the highest peak value in the velocity or energy axis represents the maximum velocity or energy in the corresponding case. Each maximum value of energy is denoted in each plot. Among these six cases, the maximum value of energy in Case C achieves an energy saturation at 5.5506 MeV. In addition, we can also find that some particles at the bottom of each plot exhibit no acceleration during the entire simulation time. Other particles with jumps from lower energy to higher energy in each plot indicate how their acceleration process occurs in the shock with time. Simultaneously, energy jumps in the corresponding case show an increasingly steep tendency with a decreasing value for the constant of scattering time in Cases A, B,

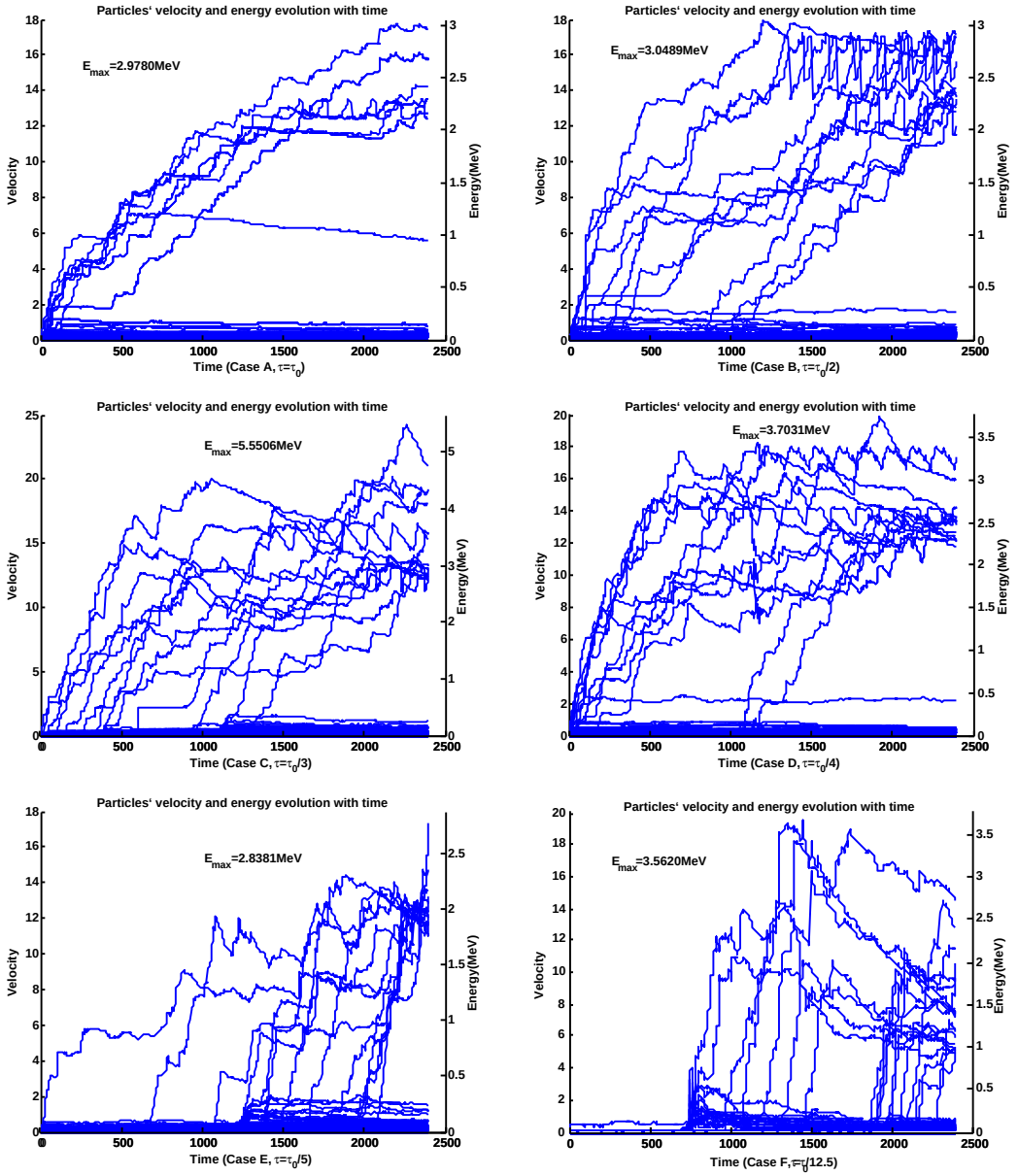

Fig. 1 A number of representative particles are extracted from the simulation box in Cases A, B, C, D, E and F. A blue curve represents one particle's evolution of velocity and energy with time. The top peak in each plot shows the maximum velocity or energy in the corresponding case. Some particles have no acceleration as indicated by lines at the bottom of each plot. A few curves with jumps from lower energy to higher energy in each plot indicate that they are accelerated in the shock with time. For comparison, the $E_{\max}$ value in Case C with a scattering time $\tau = \tau_0/3$ achieves energy saturation at 5.5506 MeV.

C, D, E and F, respectively. Case F shows very steep jumps and steep descents in energy or velocity curves because the scattering time $\tau = \tau_0/12.5$ is chosen to approach the value of the time step ($dt = \tau_0/25$). These results indicate that computational accuracy requires the scattering time to be significantly longer than the time step.

3.2 The $E_{\max}$ Function.

Here, we focus on an isolated CME-driven shock for calculating the maximum particle energy $E_{\max}$ in those cases that apply different values for scattering time. Using our dynamical Monte Carlo model, we have obtained different values for $E_{\max}$ in those cases. So, we can build the function of maximum particle energy $E_{\max}$ versus the values for the scattering time τ with values from τ_0, $\tau_0/2$, $\tau_0/3$, $\tau_0/4$ and $\tau_0/5$ to $\tau_0/12.5$ in the corresponding cases.

Utilizing the method described in Section 2, the calculations of $E_{\max}$ are performed under the scattering angular distribution with a standard deviation of $\sigma = \pi$ and an average of $\mu = 0$, which would be relatively more efficient for particle acceleration in the CME-driven shock demonstrated by the previous model (Wang & Yan 2012). From the large population of accelerated particles at the end of

the simulation in each case, we find each maximum local velocity $VL_{\max}$ in the corresponding case with its scattering time τ. The relationship between the maximum local velocity $VL_{\max}$ and the value for the scattering time τ in all cases is shown in Figure 2.

In Figure 2, the solid line denotes the correlation of the maximum local velocity $VL_{\max}$ versus the different value for the scattering time τ in the corresponding case. In the present Monte Carlo model, the value for the scattering time τ is chosen to have values τ_0, $\tau_0/2$, $\tau_0/3$, $\tau_0/4$, $\tau_0/5$ and $\tau_0/12.5$, respectively. These six squares represent the maximum local velocity values for $VL_{\max}$ in all cases with their corresponding values for the scattering time. The maximum local velocity $VL_{\max}$ is represented by a dimensionless value for $VL_{\max(A)} = 17.7824$, $VL_{\max(B)} = 17.9928$, $VL_{\max(C)} = 24.2773$, $VL_{\max(D)} = 19.8295$, $VL_{\max(E)} = 17.3596$ and $VL_{\max(F)} = 19.4482$ in each case, respectively. As shown in Figure 2, among these maximum local velocities for $VL_{\max}$, the largest is the one in Case C with a value of $VL_{\max(C)} = 24.2773$, and its value for the scattering time is $\tau_0/3$. The top of the stairstep graph in Figure 2 shows that there exists a saturation in the function of the maximum local velocity $VL_{\max}$ versus the value of the scattering time τ under the resonant diffusion scenarios.

Figure 3 shows the fitting curve of the maximum particle energy $E_{\max}$ versus the values for the scattering time τ. The maximum particle energies $E_{\max}$ are calculated in the shock frame by scaled values according to the scale factor for velocity $v_{\rm scale}$. The maximum particle energy $E_{\max}$ in each case varies along the shape-preserving curve in a sequence of $E_{\max(A)} = 2.9780$ MeV, $E_{\max(B)} = 3.0489$ MeV, $E_{\max(C)} = 5.5506$ MeV, $E_{\max(D)} = 3.7031$ MeV, $E_{\max(E)} = 2.8381$ MeV and $E_{\max(F)} = 3.5620$ MeV corresponding to Cases A, B, C, D, E and F, respectively. None of those maximum particle energies $E_{\max}$ exceed the upper limit of $E_{\rm break}$ at 10 MeV derived from observations. However, Case C with a corresponding value for the scattering time $\tau_0/3$ shows that the largest maximum particle energy is $E_{\max(C)} = 5.5506$ MeV, which is still less than the upper limit of the $E_{\rm break}$ region. It implies that whatever value for the scattering time is chosen under an isolated shock model, the maximum particle energy $E_{\max}$ would not be more than the upper limit of the $E_{\rm break}$ region in the observed energy spectrum. According to these simulation results, the energy spectrum "cut-off" would be formed near the energy of 5 MeV. In addition, the saturation value for the maximum energy function demonstrates that these maximum particle energies $E_{\max}$ can fit the observed lower energy spectrum below the $E_{\rm break}$ limit. By examining the shape-preserving curve in Figure 3, $E_{\max}$ will not increase when the value for the scattering time τ decreases from $\tau_0/3$ to $\tau_0/5$. Although the function of maximum particle energy $E_{\max}$ shows a slight rising tendency when the value for the scattering time decreases from $\tau_0/5$ to $\tau_0/12.5$, the value for the scattering time $\tau_0/12.5$ approaches the time step dt (i.e., $dt = \tau_0/25$). Considering the precision of the calculation, the value for the scattering time τ should be chosen to be not less than the time step dt. Since the amplified magnetic field is limited by the order of magnitude $\delta B/B \sim 1$, whatever value for the scattering time is chosen in an isolated shock model, the obtained maximum particle energy $E_{\max}$ is not more than the upper limit of $E_{\rm break}$ in the observed energy spectrum. If we expect to obtain a more extended energy spectrum beyond the upper limit of $E_{\rm break}$ at 10 MeV and even up to GeV, the multiple shock model would be applied. This means the efficiency of acceleration in an isolated shock model will not exceed the upper limit of $E_{\rm break}$ as long as the value for scattering time is chosen to be sufficiently greater than the time step dt. In addition, it also implies that a realistic observation of the $E_{\rm break}$ energy spectrum requires a multiple shock model to transfer the shock's energy into superthermal particles up to a highest energy spectrum for explaining the $E_{\rm break}$ formation and the higher energy spectrum.

3.3 The Energy Spectra

Figure 4 shows the shock energy spectra calculated in the downstream region in all cases. As far as the shape of the energy spectrum is concerned, the power-law slopes of six extended curves are similar, because all cases are done in the same resonant diffusion scenarios but with different values for the scattering time. However, among these cases, the energy spectrum in Case C with the value for scattering time of $\tau_0/3$ shows a relatively steep slope in the highest energy spectral tail. Under an isolated shock model, each case shows how the initial Maxwellian energy spectrum evolves into the extended energy spectrum with a "power-law" structure in its high energy range. By comparison, we calculated the average value of the maximum particle energy in the present six cases. The average value for maximum particle energy is $\langle E_{\max}\rangle = 3.6135$ MeV and the average value for energy spectral index is $\Gamma \sim 1.125$. These results agree with the low energy spectrum in terms of observations from multiple spacecraft. The observed energy spectrum (Mewaldt et al. 2008) shows a low energy spectrum with an index of $\Gamma = 1.07$ and a high energy spectrum with an index of $\Gamma = 2.45$. The observed energy spectrum indicates that there is an $E_{\rm break}$ between the lower energy spectrum and the higher energy spectrum. From these simulated cases, we conclude that all these energy spectra are characterized by a "power-law" with an average index $\Gamma \sim 1.125$, which is consistent with the observed index $\Gamma = 1.07$ of the low energy spectrum. Since there is no maximum particle energy $E_{\max}$ in these six cases beyond the upper limit of $E_{\rm break}$ at 10 MeV, we are unable to conclude that there should be an $E_{\rm break}$ at 1–10 MeV that acts as a "break" from the lower energy spectrum to higher energy spectrum at this range. If we expect the second higher energy spectrum to exist, we can speculate that there must be an enhancement in amplification of the magnetic field associated with the multiple shock model. We propose that

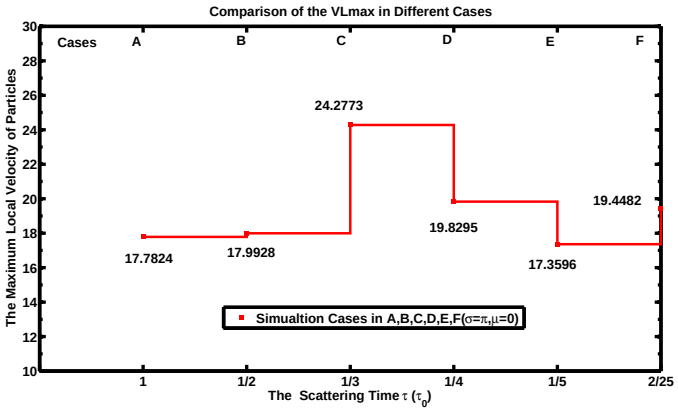

Fig. 2 The maximum local velocities $VL_{\max}$ of the accelerated energetic particles in all cases are plotted as a stairstep graph of the value for the scattering time. All these cases are simulated using a Monte Carlo model that incorporates a Gaussian scattering angular distribution with a standard deviation of $\sigma = \pi$ and average value of $\mu = 0$.

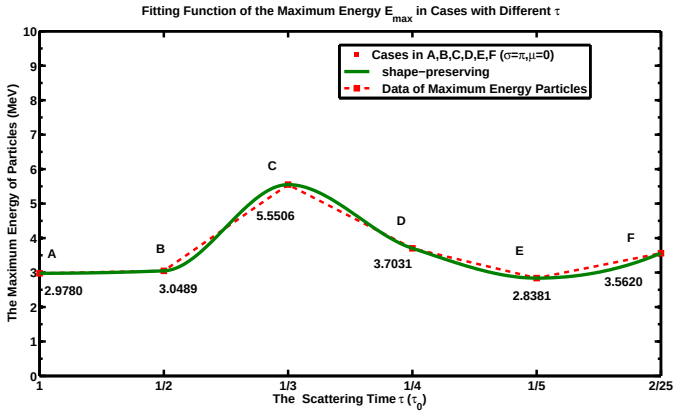

Fig. 3 The shape-preserving curve of the maximum particle energy $E_{\max}$ as a function of the value for the scattering time in six cases. The values for maximum particle energy are indicated by scaled values along the profile of the shape-preserving curve in all cases with different values for the scattering time. The profile of the $E_{\max}$ in different cases shows a saturation value for the maximum particle energy in Case C with a critical value for the scattering time $\tau_0/3$. However, none of them exceed the upper limit of $E_{\rm break}$ as derived from 10 MeV observations.

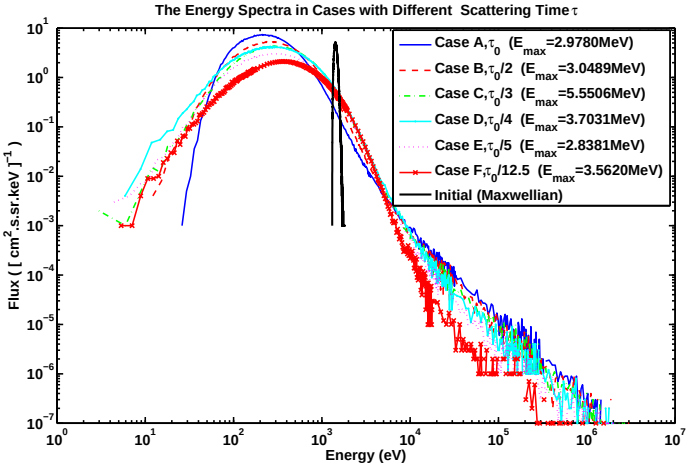

Fig. 4 The energy spectra obtained from the downstream region in six cases with different values for the scattering time. The thick solid line with a narrow peak at $E = 1.4315$ keV represents the initial Maxwellian energy distribution in the upstream region. All of cases are consistent with the low energy spectrum with all $E_{\max}$ being less than 10 MeV.

the multiple shock model should be applied to further investigate the higher energy spectrum in CME shock events.

Recently, some analyses of multiple CME collision events have been discussed. For example, Cheng et al. (2013) reported the initiation process of compound CME activity consisting of two successive eruptions of flare ropes that occurred on 2012 January 23. Another example described by Liu et al. (2014) indicates that the interactions between consecutive CMEs resulted in a "perfect storm" near 1 AU on 2012 July 23, which would induce a nonlinear amplification of the magnetic field. Also, more evidence could be gathered from observations by spacecraft such as SDO, SOHO, ACE, Wind, etc. As is implied from these simulated results, we propose building a multiple shock model to simulate the $E_{\rm break}$ formation and the higher energy spectrum in the interplanetary shock. In the present model, we think that the parameter of the scattering time would play a key role in the strength of the diffusive coefficient for production of $E_{\rm max}$ within the resonant diffusion scenarios associated with an isolated shock. According to the final results, we find a relationship between the maximum particle energy $E_{\rm max}$ and the different value for the scattering time in an isolated shock model. Although the difference in these maximum particle energies $E_{\rm max}$ in simulated cases has been observed, no maximum particle energy $E_{\rm max}$ can exceed the upper limit of $E_{\rm break}$ to further evolve into a higher energy spectrum up to GeV. More simulations in the future are necessary to verify the higher energy spectrum with an index of $\Gamma \simeq 2.5$ and the energy spectral "break" formation by applying the multiple shock model.

4 SUMMARY AND CONCLUSIONS

In summary, these presented simulations are unable to verify that there should be an energy spectral "break" below 10 MeV in some large CME-driven shocks. Instead, we verify that there is an energy spectral "cut-off" near the range of energy at 5 MeV in an isolated CME-driven shock. We calculate the maximum particle energy $E_{\rm max}$ by focusing on the 2006 Dec 14 CME-driven shock event and build the relationship between the maximum particle energy $E_{\rm max}$ and the value for the scattering time τ. We find that the maximum particle energy $E_{\rm max}$ approaches a saturation near 5 MeV below the upper limit of $E_{\rm break}$ for the observed energy spectrum. We verify that the lower energy spectrum is consistent with the observed low energy spectrum, but no higher energy spectrum appears. Although there have been several large SEP events in the past solar cycle 23 that appeared to have energy spectral "breaks" between 1–10 MeV, there is still no reasonable explanation for this. Since these observations depend on multiple spacecraft, it is not easy to treat the system errors and incorporate data obtained from different spatial orientations. The huge computational expense also limits numerical methods from reaching a sufficiently high energy spectral tail for further identification of this "break." In view of the current theoretical point about DSA, the analytic method gives an implication that this "break" would be connected with a particle leakage mechanism. This "break" seemingly can be predicted in a location outside of the shock associated with supernova remnants (SNRs), where the SNRs collide with nearby molecular clouds. This idea will motivate us to further investigate the energy spectrum $E_{\rm break}$ formation and the higher energy spectrum. Hopefully, we can investigate how the multiple shock model would play a key role in explaining the energy spectrum $E_{\rm break}$ formation and the higher energy spectral shape.

Acknowledgements The present work is supported by the Xinjiang Natural Science Foundation (No. 2014211A069). This work is also funded by the Key Laboratory of Solar Activity of NAOC, the Key Laboratory of Modern Astronomy and Astrophysics (Nanjing University), Ministry of Education, and the China Scholarship Council (CSC). The authors thank both Profs. Joe Giacalone at the University of Arizona and H. B. Hu at the Institute of High Energy Physics, Chinese Academy of Sciences, for their very helpful comments and discussions on this paper.

References

Amato, E., & Blasi, P. 2006, MNRAS, 371, 1251
Amano, T., & Hoshino, M. 2007, ApJ, 661, 190
Bell, A. R. 1978, MNRAS, 182, 147
Bell, A. R., Schure, K. M., Reville, B., & Giacinti, G. 2013, MNRAS, 431, 415
Bykov, A. M., Malkov, M. A., Raymond, J. C., Krassilchtchikov, A. M., & Vladimirov, A. E. 2013, Space Sci. Rev., 178, 599
Caprioli, D., Amato, E., & Blasi, P. 2010, Astroparticle Physics, 33, 307
Caprioli, D., & Spitkovsky, A. 2013, ApJ, 765, L20
Caprioli, D., & Spitkovsky, A. 2014, ApJ, 783, 91
Cheng, X., Zhang, J., Ding, M. D., et al. 2013, ApJ, 769, L25
Drury, L. O. 1983, Reports on Progress in Physics, 46, 973
Drury, L. O., & Voelk, J. H. 1981, ApJ, 248, 344
Ellison, D. C., Moebius, E., & Paschmann, G. 1990, ApJ, 352, 376
Ellison, D. C., & Double, G. P. 2004, Astroparticle Physics, 22, 323
Gan, W. Q., Li, Y. P., & Chang, J. 2001, ApJ, 552, 858
Gargaté, L., & Spitkovsky, A. 2012, ApJ, 744, 67
Giacalone, J., Burgess, D., Schwartz, S. J., & Ellison, D. C. 1993, ApJ, 402, 550
Giacalone, J. 2004, ApJ, 609, 452
Gopalswamy, N., Yashiro, S., Liu, Y., et al. 2005, Journal of Geophysical Research (Space Physics), 110, 9
Guo, F., & Giacalone, J. 2012, ApJ, 753, 28
Guo, F., & Giacalone, J. 2013, ApJ, 773, 158
Huang, G. 2009, Sol. Phys., 257, 323
Jokipii, J. R. 2013, Space Sci. Rev., 176, 115
Kang, H., Jones, T. W., & Gieseler, U. D. J. 2002, ApJ, 579, 337

Knerr, J. M., Jokipii, J. R., & Ellison, D. C. 1996, ApJ, 458, 641
Kong, X., Li, G., & Chen, Y. 2013, ApJ, 774, 140
Lagage, P. O., & Cesarsky, C. J. 1983, A&A, 125, 249
Li, X., Lu, Q., Chen, Y., Li, B., & Xia, L. 2010, ApJ, 719, L190
Lin, R. P., Krucker, S., Hurford, G. J., et al. 2003, ApJ, 595, L69
Liu, S., Petrosian, V., & Mason, G. M. 2004, ApJ, 613, L81
Liu, Y. D., Luhmann, J. G., Kajdič, P., et al. 2014, Nature Communications, 5, 3481
Malkov, M. A., Diamond, P. H., Sagdeev, R. Z., Aharonian, F. A., & Moskalenko, I. V. 2013, ApJ, 768, 73
Malkov, M. A., & Voelk, H. J. 1996, ApJ, 473, 347
Mewaldt, R. A., Cohen, C. M. S., Cummings, A. C., et al. 2008, International Cosmic Ray Conference, 1, 107
Niemiec, J., & Ostrowski, M. 2004, ApJ, 610, 851
Riquelme, M. A., & Spitkovsky, A. 2011, ApJ, 733, 63
Schneider, P. 1993, A&A, 278, 315
Snodin, A. P., Ruffolo, D., Oughton, S., Servidio, S., & Matthaeus, W. H. 2013, ApJ, 779, 56
Su, Y., Veronig, A. M., Holman, G. D., et al. 2013, Nature Physics, 9, 489
Vladimirov, A., Ellison, D. C., & Bykov, A. 2006, ApJ, 652, 1246
Wang, J., & Ji, H. 2013, Science China Earth Sciences, 56, 1091
Wang, X., Wang, N., & Yan, Y. 2013, ApJS, 209, 18
Wang, X., & Yan, Y. H. 2011, A&A, 530, A92
Wang, X., & Yan, Y.-H. 2012, RAA (Research in Astronomy and Astrophysics), 12, 1535
Winske, D. 1985, Space Sci. Rev., 42, 53
Zank, G. P., Rice, W. K. M., & Wu, C. C. 2000, J. Geophys. Res., 105, 25079
Zirakashvili, V. N., & Aharonian, F. A. 2010, ApJ, 708, 965